Journal of Ethnopharmacology 214 (2018) 179–189

Contents lists available at ScienceDirect

Journal of Ethnopharmacology

journal homepage: www.elsevier.com/locate/jethpharm

Neuroprotective effect of He-Ying-Qing-Re formula on retinal ganglion cell in diabetic retinopathy

Cheng Zhang[a,b], Yu Xu[b], Hor-Yue Tan[b], Sha Li[b], Ning Wang[b], Yinjian Zhang[a,*], Yibin Feng[b,*]

[a] Department of Ophthalmology, Longhua Hospital, Shanghai University of Traditional Chinese Medicine, 725 Southern Wanping Road, Shanghai 200032, China
[b] School of Chinese Medicine, The University of Hong Kong, 10 Sassoon Road, Pokfulam, Hong Kong, China

ARTICLE INFO

Keywords:
He-Ying-Qing-Re formula
Diabetic retinopathy
RGC apoptosis
Endoplasmic reticulum stress
Retinal degeneration

ABSTRACT

Ethnopharmacology relevance: He-Ying-Qing-Re Formula (HF) was empirically modified from Si-Miao-Yong-An Decoction (SD), which was recorded in the literature of Divine Doctor's Secret Transmission, and has been utilized for centuries to treat vasculopathy through clearing heat and accelerating bloodstream. HF has been used as an effective holistic treatment of diabetic retinopathy (DR) for decades and experimentally reported to ameliorate retinal condition in diabetic mice.

Aim of the study: Our study aims to investigate the effect of HF in preventing sustained hyperglycemia and hyperlipidemia-associated retinal ganglion cell (RGC) cell death and its possible mechanism.

Materials and methods: Chromatographic fingerprint of HF was obtained upon the UPLC-based analytic system; Diabetic retinopathy was established in streptozotocin (STZ) injection-induced hyperglycemic mice; Alterations of retinal structure was assayed by H&E staining. Expression of PSD-95 and CHOP in retinae was assessed by immunofluorescence; RGC cell line (mRGC) was used for in vitro study. Cell death was analyzed by flow cytometry; Intracellular reactive oxygen species (ROS) was measured by 2′,7′-dichlorofluorescin diacetate (DCFDA); Apoptosis-related proteins and signaling were monitored with immunoblotting and colorimetric assay.

Results: Chlorogenic acid, ferulic acid, and rutin were identified in HF. HF attenuates the loss of RGCs, thinning of inner retinal layers in diabetic mice. Furthermore, expressions of Brn3a and PSD-95 were restored while CHOP level was downregulated upon HF treatment. In vitro study, HF alleviates H_2O_2-induced apoptosis of mRGCs and loss of postsynaptic protein via scavenging ROS and suppressing ATF4/CHOP-mediated endoplasmic reticulum stress and mitochondria-related pro-apoptotic factors, probably as cleaved-caspase-3, and phospho-p38 mitogen-activated protein kinase (MARK). Meanwhile, both pro-survival protein levels like Bcl-2/Bcl-xL and postsynaptic protein of PSD-95 were upregulated upon HF treatment.

Conclusion: HF administration was a valid therapeutic approach for DR treatment, oriented at the blockade of endoplasmic reticulum- and mitochondria-dependent oxidative stress-induced retinal neurodegeneration including RGC apoptosis.

1. Introduction

Diabetic retinopathy (DR) is characterized by progressive neurological deficits associated with concomitant retinal microvascular degeneration that contributes to the inevitable and permanent visual dysfunction (Kim et al., 2016; Ng et al., 2016). In accordance with the recent trend in epidemiological-clinical twin study of DR, the diabetic population worldwide will be approximately increased to 500 million by 2030 (Whiting et al., 2011). Accordingly, numerous ophthalmic therapies aimed at alleviation of hyperglycemia-induced retinopathy have been proposed, including laser photocoagulation, vitrectomy and intravitreal injection of anti-VEGF agents (Lee et al., 2015; Singh et al., 2014; Tremolada et al., 2012). However, the aforementioned curative interventions, which possess remarkable effects in arresting the

Abbreviations: HF, He-Ying-Qing-Re Formula; RGC, Retinal ganglion cell; DR, Diabetic retinopathy; STZ, Streptozotocin; GCL, Ganglion cell layer; INL, Inner nuclear layer; IPL, Inner plexiform layer; H_2O_2, Hydrogen peroxide; ROS, Reactive oxygen species; BRB, Blood-retinal barrier; ATF4, Activating transcription factor 4; CHOP, C/EBP homologous protein; PSD 95, Postsynaptic density protein 95; SD, Si-Miao-Yong-An Decoction; FBG, Fasting blood glucose; RBG, Random blood glucose; IPGTT, Intraperitoneal glucose tolerance test; AUC, Area under the curve; Cyt-C, Cytochrome C; IGF-1, Insulin-like growth factor-1; HIF-1α, hypoxia-inducible factor 1α; MAPK, mitogen-activated protein kinase; ROS, reactive oxygen species; DCFDA, 2′,7′-dichlorofluorescin diacetate

* Corresponding authors.
E-mail addresses: zttc@connect.hku.hk (C. Zhang), u3004614@connect.hku.hk (Y. Xu), hyhtan@hku.hk (H.-Y. Tan), u3003781@connect.hku.hk (S. Li), ckwang@hku.hk (N. Wang), zhangyinj@126.com (Y. Zhang), yfeng@hku.hk (Y. Feng).

https://doi.org/10.1016/j.jep.2017.12.018
Received 25 September 2017; Received in revised form 28 November 2017; Accepted 14 December 2017
Available online 15 December 2017

deterioration of retinal detachment, neurodegeneration, and neovascularization, are insufficient to prevent visual impairment. This majorly caused by the limitation of specific therapeutic targets and unavoidable side-effects, such as peripheral vision loss, worsening of macular edema and reduction in night vision in parallel with the deficiency of contrast sensitivity. Therefore, alternative pharmacological therapies for DR treatment that not affecting the visual functions are urgently demanded.

Growing evidence has demonstrated that prevailing diabetes-induced complications have been alleviated with minimal side-effects via the treatment of herbal medicines (Watal et al., 2014). Meanwhile, more than 200 kinds of traditional medicinal plants as well as their bioactive compounds are documented to possess anti-diabetic property as illustrated via substantial screening methods (Yang et al., 2013c). He-Ying-Qing-Re Herbal Formula (HF) was empirically modified from Si-Miao-Yong-An Decoction (SD), which has been utilized for centuries to treat patients with vasculopathy through clearing heat and accelerating blood stream with ingredients of Lonicera japonica, Glycyrrhiza uralensis, angelica sinensis and scrophularia, based on the traditional Chinese medicine theory from the literature of “Shen-Yi-Mi-Zhuan” (Divine Doctor's Secret Transmission) written by Hua Tuo (A.D. 141–203), a renowned Chinese herbalist as “Medical Sage” in the Han Dynasty of China (Liu et al., 2017b; Yang et al., 2013a). In the contemporary era, SD has experimentally reported to relieve diabetes with retinal hemorrhage, feet syndrome as well as atherosclerotic upon downregulating such expressions as TNF-α, IL-6, IL-8 and lipid levels in blood (Cui et al., 2009; Yang and Liu, 2008; Zhang et al., 2010) The optimized formula of HF derived from SD was first created and clinically used by Dr. Jusheng Zhou, an experienced expert in traditional Chinese medicine at Longhua hospital of Shanghai, and shown beneficial for improving visual function with no reported ineluctable side-effects for decades (Ye and Zhang, 2012), suggesting that HF tended to possess certain anti-DR characteristics.

It has been postulated that apoptosis of retinal ganglion cell (RGC), a pathological and predominant hallmark of neurodegeneration in DR, is involved in the progressive but irreversible reduction of the thickness of inner retinal layer and vision loss (Adamiec-Mroczek et al., 2015). The cross-sections of endoplasmic reticulum stress and mitochondria-dependent oxidative stress to the diabetes-induced retinal pathology are responsible for the acceleration of RGC apoptosis (Jia et al., 2014; Wang et al., 2016). Conventionally, the activation of oxidative- and/or endoplasmic reticulum-stress in retinal neural cells, including RGC, can be induced by hyperglycemia-generated hydrogen peroxide (H_2O_2), an endogenous reactive oxygen species (ROS), which also instigates the onset of degenerative cascade of microvasculature involving breakdown of blood-retinal barrier (BRB) (Fan et al., 2016; More et al., 2017). The misfolded or unfolded protein response can be accumulated in the lumen of endoplasmic reticulum owing to the interruption of the protein folding triggered by numerous stimuli, including overexpression of H_2O_2 (Zhang and Kaufman, 2004). For example, up-regulation of the activating transcription factor 4 (ATF4) transcription could facilitate the stimulation of potential downstream substrates such as transcriptional factor C/EBP homologous protein (CHOP) and post-synaptic density protein 95 (PSD 95) (Hetz, 2012; Wang et al., 2016; Xu et al., 2005). In addition, the phosphorylation of p38 mitogen-activated protein kinase (p38 MAPK) as well as the inactivation of pro-survival Bcl-2 family members, are all involved in the initiation of endoplasmic reticulum- and/or oxidative-stress (Sano and Reed, 2013). Although inhibiting the expression of aforementioned proteins may reduce RGC apoptosis, consensus on the proverbial pharmacological targets for the alleviation of apoptosis-associated DR progression have not been cleared. Therefore, a promising therapeutic strategy, based on the attenuation of H_2O_2-induced endoplasmic reticulum- and/or oxidative-stress, is worthy to be considered in combating RGC apoptosis in DR progression.

Our previous study has showed that HF elicited beneficial effects on the inhibition of advanced glycation end products generation via up-regulating the expression of tight junction proteins, Zo-1 and Claudin-1, of which factors lead to the decrease of fundus lesions such as hemorrhages, exudation and edema (Wang et al., 2015; Zhang et al., 2012). Nonetheless, the clear mechanism of HF in neuroprotection of DR-induced vision loss remains elusive. To clarify these above-mentioned considerations, the present study aimed to investigate the potential protective effects of HF on RGC apoptosis associated with microvascular degeneration caused by H_2O_2-induced endoplasmic reticulum- and mitochondria-dependent oxidative stress, using the transformed mouse RGC cell line (mRGC). In parallel, STZ, a natural chemical toxic to pancreatic β-cells, is adopted to establish insulin-deficient diabetic mice. We have taken advantage of multiple assessment approaches to elucidate the postulated properties of HF against DR both in vitro and in vivo.

2. Materials and methods

2.1. Preparation of HF extract

HF consists of eight herbs and the mixed proportion of respective herb in HF is illustrated in Fig. 1A–B. All the mentioned herbal names can be checked in accordance with the database of www.theplantlist.org (Fig. 1C). Raw herbs were obtained from the pharmacy of School of Chinese Medicine (SCM), the university of Hong Kong (HKU), authenticated by the executive manager of pharmacy dispensary of HKU. Voucher specimens with specific storage code were well-deposited at SCM, HKU. 10 times of ddH_2O (w/v) was added and boiled twice for one hour each time. The raw drug liquid was concentrated with a final concentration of 2 g dried crude herb per ml. HF extract was filtered and stored in − 80 °C until used.

2.2. Chromatographic fingerprint analysis

Ultra Performance Liquid Chromatography (UPLC) (Thermo Fisher Scientific, USA) system was utilized for the identification and separation of sample components in HF, corresponding to the relative absorbance and peak time of known standard compounds, including chlorogenic acid, ferulic acid, caffeic acid, acteoside and rutin (TAUTO, China), and aimed to capture as many peaks as possible (Fig. 2A). C18 column (100 mm × 2.1 mm id) (ACE, UK) was used as solid phase and the column temperature was maintained at 30 °C. Meanwhile, the mobile phase contains binary solvent mixture of acetonitrile and 0.05% KH_2PO_4 (PH = 2.5). The chromatographic gradient elution procedure is illustrated in Fig. 2B while the monitoring wavelength is 330 nm with a flow rate of 0.5 ml min^{-1}.

2.3. Animals interventions and Streptozotocin-induced DR model

Experimental procedures in this study were performed according to the approved protocol of Committee on the Use Research (CULATR) (Certificate Number: 3354-14) and ethical guidelines of Laboratory Animal Unit affiliated to The University of Hong Kong (LAU, HKU) for the use of laboratory animals. Male mice (C57BL/6N) ranging from 6 to 8 weeks of were purchased from LAU and housed in animal units in LAU as well, which were placed under a 12 h light/dark schedule and given free access to the food and water. Diabetic mice were established via 5 consecutive intraperitoneal injections of streptozotocin (STZ; 55 mg/kg), which dissolved in citrate buffer (pH 4.5) (Sigma USA). After 3 days of operation, mice with blood glucose lower than 15 mmol/l measured by a glucometer (Contour TS, Bayer, Germany) were eliminated from this study. STZ-induced hyperglycemic mice were randomly separated into four groups. Initially, insulin-treated (Humulin, USA; 1 U/kg; n = 5) and untreated diabetic mice (n = 5) are regarded as positive control and model group respectively. On the other hand, the remaining mice with hyperglycemia received HF via daily

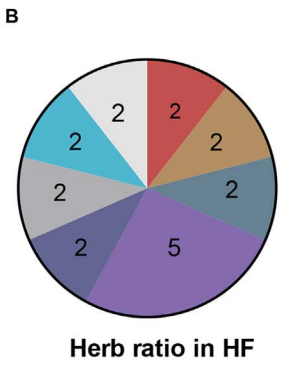

C

Botanical name	Herbal name	Chinese name	Voucher NO.	Ratio in HF
Arctium lappa L.	Fructus Arcti	Niu-Bang-Zi	SCM16P05231	2
Taraxacum mongolicum Hand. -Mazz	Herba Taraxaci	Pu-Gong-Ying	SCM16P05232	5
Polygonatum sibiricum F.Delaroche	Rhizoma Polygonati Cyrtonematis	Huang-Jing	SCM16P05233	2
Rehmannia glutinosa (Gaertn.) Libosch. ex Fisch. & C.A. Mey.	Radix Rehmanniae Exsiccata	Sheng-Di	SCM16P05234	2
Lycium barbarum L.	Fructus Lycii Babari	Gou-Qi-Zi	SCM16P05235	2
Scrophularia ningpoensis Hemsl.	Radix Scrophulariae	Xuan-Shen	SCM16P05236	2
Angelica sinensis (Oliv.) Diels.	Radix Angelicae Sinensis	Dang-Gui	SCM16P05237	2
Lonicera japonica Thunb.	Flos Lonicerae	Jin-Yin-Hua	SCM16P05238	2

Fig. 1. Information of components in He-Ying-Qing-Re Formula (HF). (A) Representative figures of herbs in HF. (B) Ratio of each herb in HF. (C) List of accepted Botanical, Herbal and Chinese name of the corresponding herb in HF with its voucher number according to www.theplantlist.org.

gavage with two doses, 50 mg/kg (low dose; n = 5) and 100 mg/kg (high dose; n = 5) respectively. Untreated non-diabetic mice were utilized as normal control and daily given ddH_2O as a model group. Mice were sacrificed with overdose of pentobarbital (200 mg/kg) injection once DR established.

2.4. Assessment of fasting, random blood glucose, intraperitoneal glucose tolerance test and weight

To verify the hypoglycemic efficacy of HF in DR treatment, fasting blood glucose (FBG), random blood glucose (RBG) and intraperitoneal glucose tolerance test (IPGTT) were measured with the same glucometer (Bayer, Germany). We performed weight once a week and FBG measurements every 4 weeks respectively, while RBG was monitored at 3 days followed by 2 or 4 weeks after the last STZ injection. For IPGTT measurement, mice were assigned to go through a persistent 12-h fasting program followed by FBG measurement as baseline initially followed by the assessment at 0.5, 1, 1.5, 2 h after blood glucose (2 g/kg) injection. The area under the curve (AUC) evaluated the glucose tolerance ability of mice, which was plotted by linking 5-time points in each group.

2.5. Quantitative assessment of RGC loss and inner retinal layer thickness

Paraffin-embedded section technology combined with H&E staining was utilized to observe the pathological changes of RGC loss and retinal structure degeneration in DR mice. Briefly, mice were euthanized with overdose-injection of pentobarbital (200 mg/kg) and eyes were enucleated immediately followed by fixation with 4% PFA for 24 h. Then, eyeballs were immersed in 70%, 80%, 90%, 95% ethanol once an hour for gradient dehydration. Subsequently, eyecups were taken seriously and immersed in 95% ethanol for 30 min followed by incubation with 100% ethanol for 10 min each. Afterwards, eyes were embedded with paraffin and slid into sections (5 μm thick) along the vertical meridian followed by deparaffinization and rehydration with xylene and graded ethanol series (70%, 90%, and 100%) including H&E staining respectively. Images were captured with a digital microscope (EVOS, USA) at 400× magnification. Quantifications of the number of RGCs and the

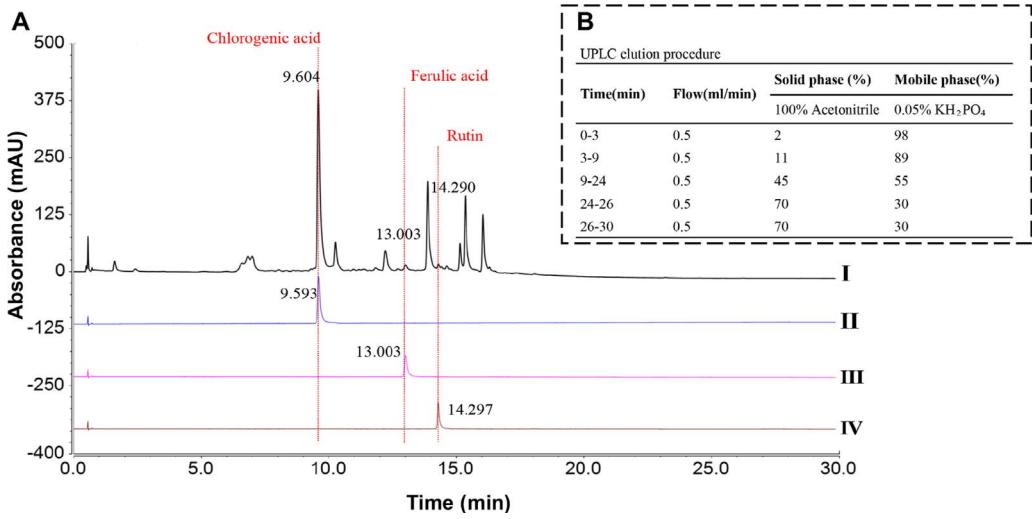

B

UPLC elution procedure

Time(min)	Flow(ml/min)	Solid phase (%)	Mobile phase(%)
		100% Acetonitrile	0.05% KH_2PO_4
0-3	0.5	2	98
3-9	0.5	11	89
9-24	0.5	45	55
24-26	0.5	70	30
26-30	0.5	70	30

Fig. 2. Chromatographic fingerprinting of HF and standards, using a gradient elution procedure. (A)Chromatograms of HF and standards with labeled peak time respectively. I: chlorogenic acid; II: Ferulic acid; III: Rutin (B) Detailed procedure of UPLC gradient elution program.

thickness of the ganglion cell-, inner nuclear- or inner plexiform layer were performed in eight randomly selected vision fields with an identical area of 0.076 mm^2 (275 × 275 μm), captured with a reference micrometer in a microscope (Olympus BX43, Australia) under the same conditions. The measurement of inner retinal layers was quantified with Image J processing program (National Institute of Health, USA).

2.6. Immunofluorescence analysis

The approaches for the preparation of paraffin-embedded retinal slice were consistent with the methods described above. Deparaffinized and rehydrated sections were heated in a 10 mM citrate buffer (pH 6.0) for 1–2 min in a microwave oven for the procedure of antigen retrieval. Subsequently, sections were rinsed with deionized water followed by incubation with 1% H_2O_2 dissolved in PBS for 5 min. Then, samples were immersed in blocking buffer, containing 10% bovine serum albumin and 0.3%Triton X-100 in PBS, for 2 h and incubated with respective anti-PSD 95 or anti-Brn3a primary antibody (1:300 dilution; Abcam, UK) overnight at 4 °C. Thereafter, sections were infiltrated with appropriate secondary antibody conjugated with Alexa-Fluor-488 or -568 (1:500 dilution; Invitrogen, USA) and counterstained with DAPI. Images were visualized and captured randomly with a confocal laser microscope at 200× magnification (Carl Zeiss LSM 780, USA).

2.7. Cell culture and assessment of cell viability

mRGC cell, a cell line derived from mouse retinal ganglion cells, was obtained from Ying-Run Biotechnology Inc. (Changsha, China) and routinely maintained in DMEM supplemented with high glucose (4.5 g/L), 10% fetal bovine serum, 100 U/ml penicillin and 100 g/ml streptomycin (Gibco, USA). Cells were cultured at 37 °C in a humidified incubator containing 5% CO_2 and 95% air and passaged until cells reach their confluence of 80%.

mRGC cell viability was analyzed via MTT assay after different interventions (Sigma, USA). Briefly, cells were seeded in 96-well plates at cell density of 1.0×10^4 per well followed by 24 h of attachment. Then, cells were cultured with different concentrations of HF or H_2O_2 simultaneously or alternatively for 24 or 48 h respectively. Thiazolyl Blue Tetrazolium Bromide (MTT, 5 mg/ml) in PBS was added to each well and incubated for another 4 h at 37 °C. Afterwards, supernatants were discarded and 100 μl DMSO was added to dissolve the crystal violet. Eventually, plate was gently vortexed for 5 s and measured at 575 nm using the BIO-RAD 680 microplate reader (Thermo Fisher Scientific, USA). Experiments were performed in five replicates.

2.8. Flow cytometry analysis of cell apoptosis

To identify and evaluate the number of apoptotic mRGCs after different interventions, cells were collected and resuspended in 1x Binding Buffer after washed twice with sterile PBS. Cells were fluorescently stained with 5 μl of PE Annexin V and 5 μl 7-AAD followed by incubation for 15 mins in the dark according to the instructions of PE Annexin V Apoptosis Detection Kit (BD Biosciences). The number of viable or apoptotic cells were analyzed by Flow Cytometer (BD, USA).

2.9. Measurement of Caspase-3 activity

Caspase-3 activity was measured with a Caspase 3 Colorimetric Assay Kit (Bio Vision, USA) following the manufacturer's instructions. Protein extraction of mRGCs was harvested followed by proteolytic reaction. Cleavage of the DEVD-*p*NA fluorophore was read in the BIO-RAD 680 microplate reader at the wavelength of 405 nm. Caspase 3 activity was determined by comparing the results with the relative absorption of the untreated control.

2.10. Measurement of cellular ROS production

ROS levels were detected in mRGCs with the probe DCFDA according to the procedures from the manufacturer (Abcam, USA). Briefly, cells were seeded on a dark, opaque-bottomed 96-well plate at the density of $2.5*10^5$. After 24 h attachment, the supernatant was discarded and cultured for 45 min in 1× Buffer with 100 μM DCFDA per well at 37 °C. Afterwards, DCFDA solution was removed followed by the addition of 1 × PBS. The fluorescence yield level, which is identical to the intracellular ROS content, was analyzed using a fluorescence plate reader at Ex/Em = 485/535 nm (BMG LABTECH, Germany) and expressed as the percentage of untreated control.

2.11. Western Blot analysis

Ice-cold radioimmunoprecipitation assay (RIPA) buffer was utilized to lyse samples for 30 min at 4 °C followed by centrifugation in a microcentrifuge at 12,000 rpm at 4 °C for 20 min 50 μg of cellular protein mixed with loading dye was separated by electrophoresis on 10% or 12% SDS-PAGE and electroblotted onto polyvinylidene fluoride membrane (PVDF, Bio-Rad). PVDF membrane was then transferred to blocking buffer containing 5% bovine serum albumin for 2 h followed by incubation with relevant primary antibodies, anti-Phosphor-p38 MARK, -CHOP, -Bcl-2, -Bcl-xL, -GAPDH (CST, USA), -ATF4 and -PSD-95 (Abcam, UK), with gentle shaking overnight. Afterwards, the membrane was incubated with secondary antibody for 2 h at room temperature. Immunoreactive bands were visualized by ECL select kit (GE Healthcare, Germany) while band intensities images were captured and quantified by a chemiluminescence imaging system (Bio-Rad ChemiDoc XRS+, USA).

2.12. Statistical analysis

All data were analyzed using SPSS software (version 18.0; SPSS Inc., USA) and presented as the means ± standard deviation (SD) throughout the test. Unpaired Student *t*-test or Mann-Whitney test was utilized to the comparison between two groups, while one-way analysis of variance (ANOVA) with Bonferroni post-test or Kruskal-Wallis test was performed to assess the comparison of more than two groups. A value of $P < 0.05$ was regarded as a significant difference.

3. Results

3.1. Chromatographic fingerprinting analysis of HF

Qualitative assessment of ingredients in HF extract was tentatively characterized by UPLC system and its chromatographic fingerprint was established as illustrated in Fig. 2B. Approximately 12 chromatographic peaks were identified as the characteristic profile in HF. Among them, three isolated compounds were identified in comparison with the UV–visible absorption spectra and retention time of the selected standards, including chlorogenic acid, ferulic acid and rutin.

3.2. HF might not impede weight loss and exhibit a remarkable hypoglycemic effect on STZ-induced diabetic mice

Metabolic dysfunction, caused by increased-glucose level, resulted in weight loss for patients with type 1 diabetes and contributing to the deterioration of DR. Hypoglycemic is deemed as a predominant therapeutic strategy for DR treatment. However, our present data showed that HF could not induce a striking hypoglycemic effect on DR mice, which is consistent with our previous findings (Wang et al., 2015). As shown in Fig. 3A-E, neither low nor high dose administration of HF leads to RBG reduction (Fig. 3C, P all > 0.05 *vs.* model). Insulin, a common anti-diabetic agent could significantly prevent hyperglycemia, as observed from the results of RBG, FBG, IPGTT, AUC (Fig. 3B-E, *P*

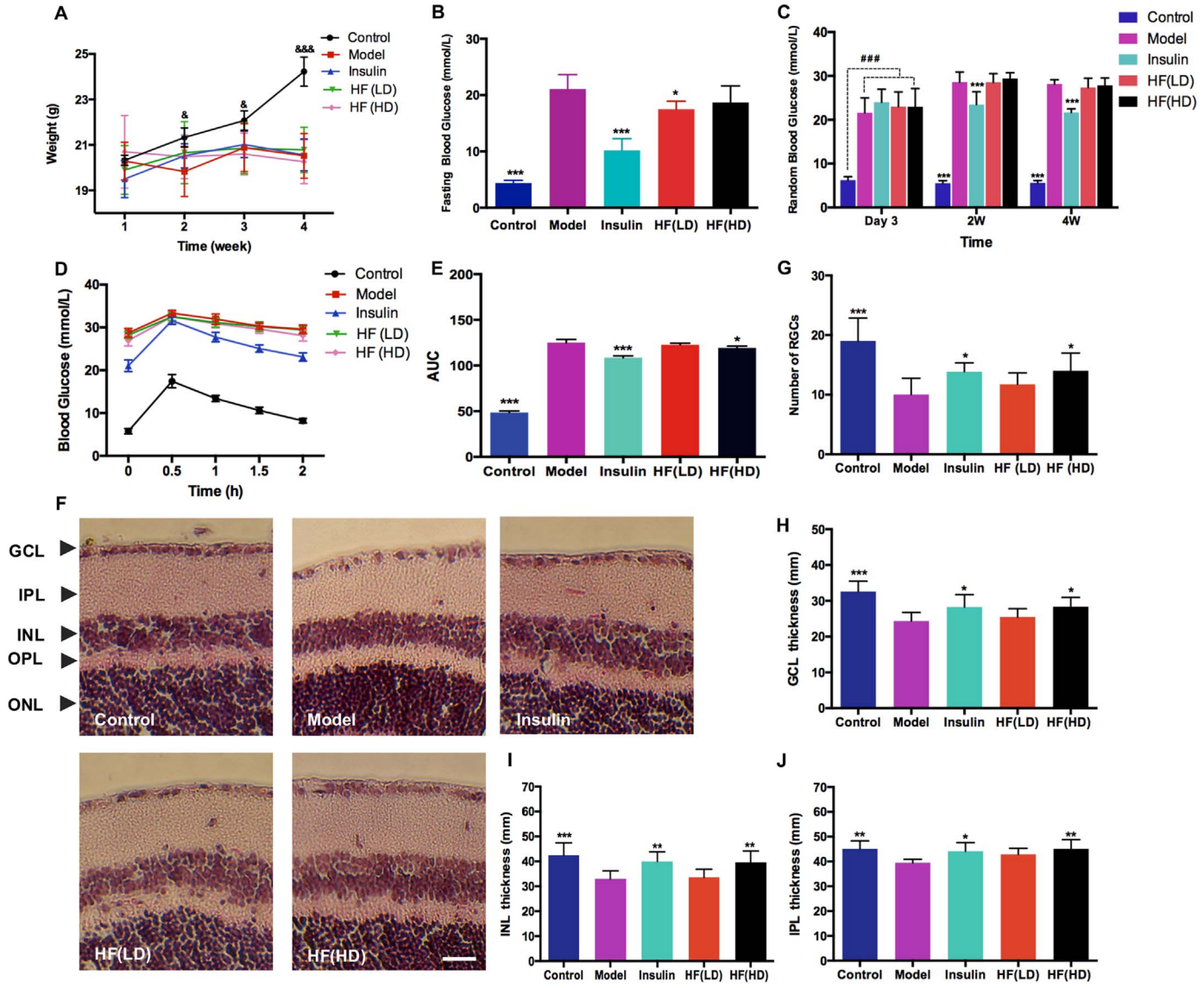

Fig. 3. HF administration might not significantly block STZ-induced hyperglycemia and weight loss but protect loss of RGCs and retinal structure degeneration in diabetic mice. (A) Changes of body weight. (B) Detection of fasting blood glucose. (C) Quantification of random blood glucose from D3 onwards after different interventions. (D, E) Intraperitoneal glucose tolerance test and its related areas under the curve (AUC) in diabetic mice with 8-week treatment, respectively. (F) H&E staining of retinal histologic sections. GCL: ganglion cell layer; IPL: inner plexiform layer; INL: inner nuclear layer; OPL: outer plexiform layer; ONL: outer nuclear layer. (G) Quantification of H&E stained RGC cells. (H-J) Measurement of thickness of GCL, INL, and IPL with H&E staining respectively. All data are presented as mean ± S.D. HF (LD): HF 50 mg/kg; HF (HD): HF 100 mg/kg. (*) $P < 0.05$ (**) $P < 0.01$ and (***) $P < 0.001$ versus Model. ($^{\#\#\#}$) $P < 0.001$ versus Control. ($^{\&}$) $P < 0.05$ and ($^{\&\&\&}$) $P < 0.001$ Control versus Model. Scale bar, 50 μm for all images.

all < 0.001 *vs*. model), without inducing regression of weight loss in STZ-induced diabetic mice (Fig. 3A, $P > 0.05$ *vs*. model). Whereas, HF was not as effective as insulin was in hypoglycemic action. Low-dose HF treatment elicited beneficial function on lowering FBG ($P < 0.05$ *vs*. model), but a weak effect on the amelioration of glucose tolerance, RBG and weight loss (P all > 0.05 *vs*. model). High-dose HF administration improved the sensitivity of glucose tolerance ($P < 0.05$ *vs*. model), but associated with ineffective control of weight loss ($P > 0.05$ *vs*. model). Our findings validated that HF might be incapable of inducing hypoglycemic activity as well as preventing weight loss for DR treatment.

3.3. High-dose of HF inhibited the reduction of inner retinal layer thickness and loss of RGC in STZ-induced diabetic mice

The majority of correlative research studies reported that patients and mammals undergoing DR lead to the degeneration of neuronal structure in retinae such as the decrease of the thickness of ganglion cell layer (GCL), inner nuclear layer (INL), inner plexiform layer (IPL) and progressive loss of RGCs (Choi et al., 2017; van Dijk et al., 2010). We quantified the number of RGCs and measured the thickness of GCL, INL, and IPL in H&E stained retinal sections (Fig. 3G–J). The considerable loss of RGCs in GCL is observationally detected in untreated diabetic mice, which could be reversed via insulin and high-dose HF treatments (P all < 0.05 *vs*. model). Furthermore, quantitative measurement illustrated a trend of thickness reduction of GCL, INL, IPL in model mice, with significant alterations emerged in the insulin and high-dose HF treated groups, as compared to that of model group (P all < 0.05). In addition, the protective actions against the reduction of GCL, INL, IPL thickness as well as the loss of RGCs were not remarkable upon low-dose HF treatment, compared with untreated diabetic mice ($P > 0.05$). In regard to these outcomes, HF might be deemed as a promising treatment option to reduce the thinning of the thickness of GCL, INL, IPL associated with attenuation of RGC loss in the progression of DR.

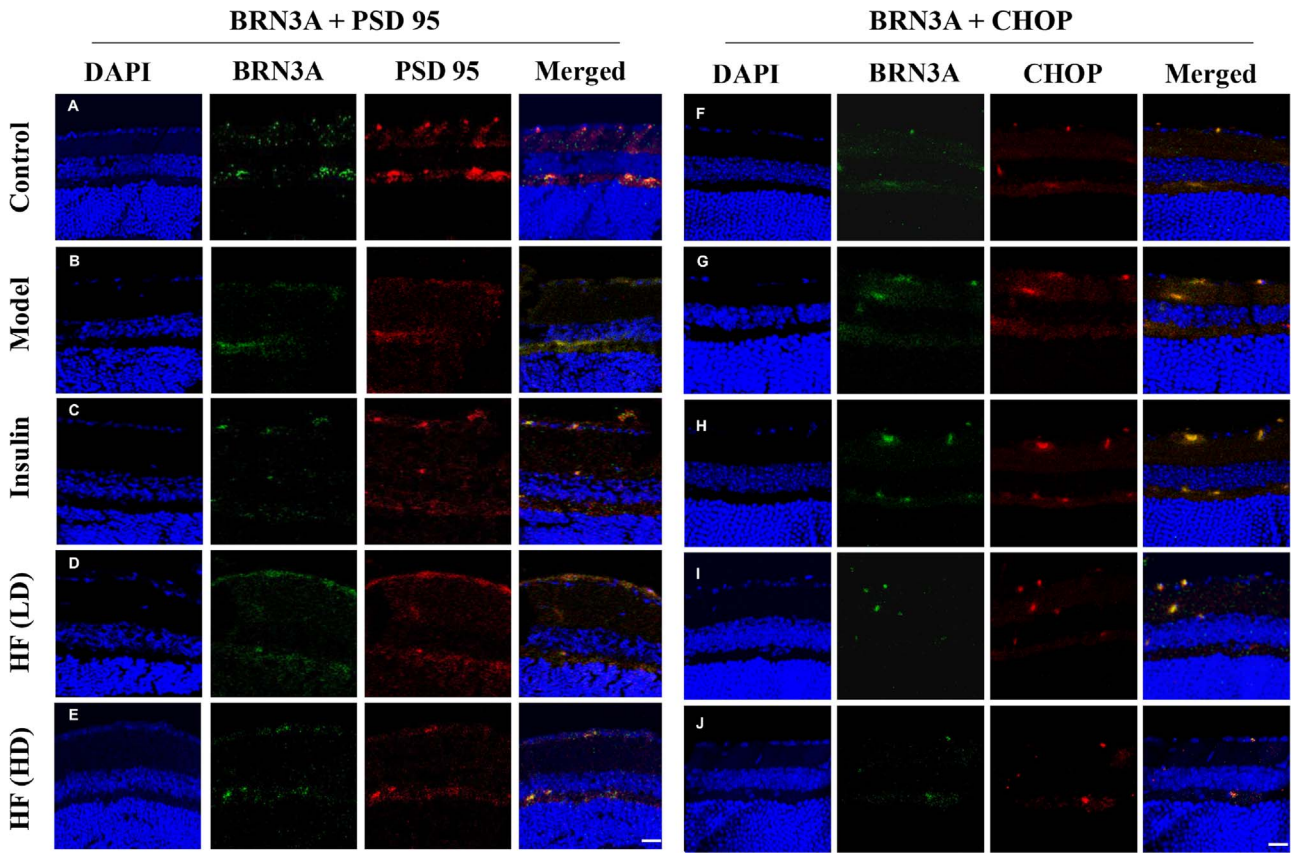

Fig. 4. HF administration attenuates the decrease in the number of Brn3a- and PSD 95- positive signaling associated with promoting the reduction of CHOP-positive RGCs in diabetic mice. (A-J) Representative confocal microphotographs of retinal tissues from untreated or STZ-induced diabetic mice after different interventions as described above. Retinal slices were immunostained with Alexa Fluor 488 (green) or Alexa Fluor 568 (red) to visualize the conjoined expression of Brn3a (green) and PSD 95/CHOP (red) in each group respectively. RGCs were specifically labeled with Brn3a that located in the GCL of retinae. Merged images show the colocalization of Brn3a and PSD 95/CHOP (red) accompanied with DAPI-stained cell nuclei (blue) in retinae. HF (LD): HF 50 mg/kg; HF (HD): HF 100 mg/kg. Scale bar, 50 μm for all images. (For interpretation of the references to color in this figure legend, the reader is referred to the web version of this article.)

3.4. HF restored expression of Brn3a and PSD 95 proteins accompanied with the enhancement of CHOP protein expression in retinae of diabetic mice

To further shed light on the underlying mechanisms of HF for the reduction of RGC loss, a confocal laser is utilized to visualize PSD 95-, Brn3a- and CHOP-positive RGCs. Sustained diminishing in the expression of PSD 95 protein and RGC-specific marker Brn3a associated with the accelerated expression of CHOP illustrated the pathological stage of RGCs undergoing neurodegenerative alternations in parallel with cell apoptosis (Nadal-Nicolas et al., 2009; Wang et al., 2016). Dramatically declined expressions of PSD 95-, Brn3a- and DAPI- positive signals in GCL of untreated diabetic mice (Fig. 4B) compared with untreated nondiabetic mice (Fig. 4A). This may account for the striking loss of RGCs and postsynaptic dendrites reflected by the sparse DAPI-stained cell nuclei of RGCs. Compared with untreated diabetic mice, no obvious decrease in the number of PSD 95- or Brn3a-labeled RGCs was observed in HF-treated diabetic mice (Fig. 4D–E), which are similar to those with insulin treatment (Fig. 4C). Furthermore, CHOP, a specific protein on behalf of the activation of endoplasmic reticulum- or ROS-stress mediated apoptosis, was expressed at low levels with Brn3a under the physiological condition in high-dose HF treatment group (Fig. 4F, J), while CHOP/Brn3a-colocalized RGCs were massively detected in untreated DR mice (Fig. 4G). In contrast, faintly RGCs stained with CHOP and Brn3a coupled with the loss of DAPI-stained RGCs were detectable in insulin or low-dose HF treated DR mice. Thus, we further confirmed that HF administration protected the decreased number of RGCs from apoptosis and the absence of postsynaptic proteins via the restoration of Brn3a and PSD 95 protein expression and downregulation of CHOP levels in retinae of STZ-induced diabetic mice.

3.5. HF attenuated H_2O_2-induced mRGC cell death

To evaluate the inhibitory action of HF on the alleviation of H_2O_2-induced mRGC death, quantification of viable mRGC cells after corresponding interventions was assessed by MTT assay. The survival rate of mRGCs cultured with H_2O_2 was decreased in a dose-dependent manner (Fig. 5A). It is demonstrated that the half maximum inhibitory concentration (IC_{50}) of H_2O_2-treated mRGC for 24 h is about 0.236 mM, equivalent to its $\log_{10}$-IC50 value is − 0.628. Thus, incubation of H_2O_2 with the optimal concentration of 0.236 mM for 24 h was adopted for subsequent in vitro experiment to evaluate the anti-apoptotic effect of HF on H_2O_2-induced mRGC damage. Next, the cytotoxicity of HF alone on mRGC cell viability was examined by exposing mRGCs to numerous concentrations (0–800 μg/ml) of HF for 24 h. HF stimulation up to 400 μg/ml did not elicit a potent cytotoxic effect, whereas statistically significant negative response was detected at 600 and 800 μg/ml, as compared to control group (Fig. 5B).

Furthermore, we explored whether HF protects H_2O_2-induced RGC cell death in DR by co-administering 0.236 mM H_2O_2 and increasing dose of HF (13–400 μg/ml) to mRGCs simultaneously or alternately. Initially, mRGC co-treated with HF and H_2O_2 at the same time elicited an inhibitory action on mRGC death, but the neuroprotection of accelerating RGC survival is relatively minor (Fig. 5C), compared to the profound inhibitory effect measured by HF pretreatment for 24 h (Fig. 5D). It was noteworthy that pretreatment with the dose higher than 100 μg/ml of HF for 24 h did not exhibit improvement on H_2O_2-

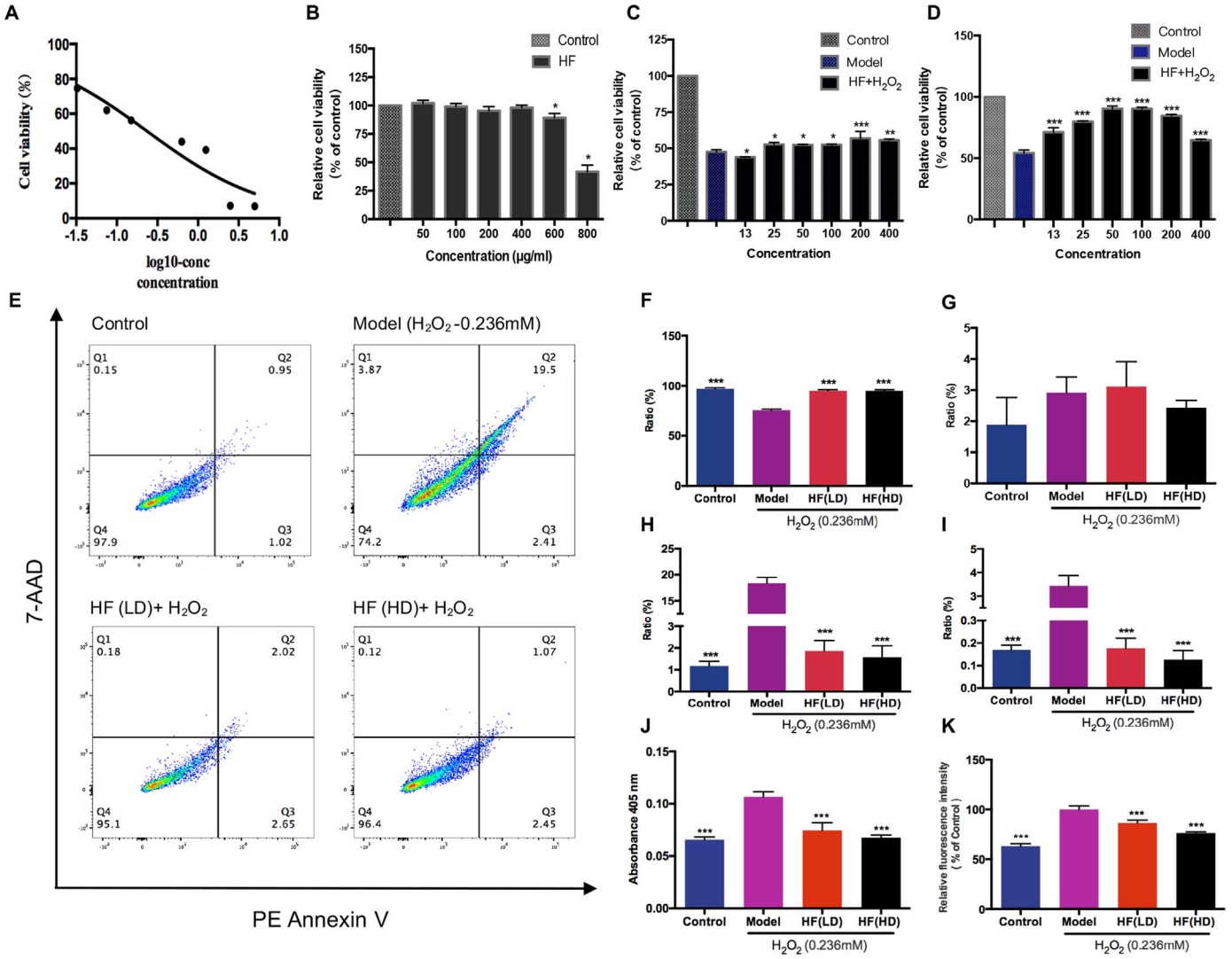

Fig. 5. HF attenuates H_2O_2-induced mRGC cell death and apoptosis via downregulation of cleaved Caspase-3 and ROS generation, analyzed by MTT assay and flow cytometer. (A) mRGC cell viability upon H_2O_2 treatment for 24 h, H_2O_2 concentrations are converted to its corresponding log10 equivalents. (B) Stimulation of mRGCs to media alone (Control) or different concentrations (50–800 μg/ml) of HF for 24 h, respectively. Cell viability is expressed as percentages of control. (C) mRGCs cultured with media and H_2O_2 (0.236 mM) for 24 h (Model) or co-treated with an increasing amount of HF (13–400 μg/ml) and H_2O_2 simultaneously for 24 h (HF+ H_2O_2). (D) Incubation of mRGCs with media or H_2O_2 (0.236 mM) for 48 h (Model) or pre-treated with HF (13–400 μg/ml) for 24 h followed by 0.236 mM H_2O_2 post-treatment for another 24 h (HF + H_2O_2). (E) Detection of mRGC apoptosis assessed by flow cytometry using double-immunostaining PE-Annexin V and 7-ADD. mRGCs were untreated (top left), treated with 0.236 mM H_2O_2 for 48 h (top right) or either pretreatment with low (bottom left) or high dose (bottom right) of HF for 24 h followed by 0.236 mM H_2O_2 incubation for another 24 h. (F-K) Average percentage of mRGCs in respective stage, according to the four quadrants of each contour diagram in Fig. 2(E). (F) viable cell. (G) early apoptotic cell (H) late apoptotic cell (I) necrotic cell. (J, K) Caspase-3 activity and ROS generation of mRGCs after pretreated with HF for 24 h followed by 0.236 mM H_2O_2 treatment for 24 h. All data are presented as mean ± S.D. based on three independent experiments. HF (LD): HF 25 μg/ml; HF (HD): HF 50 μg/ml. (*) $P < 0.05$, (**) $P < 0.01$ and (***) $P < 0.001$ versus Model.

induced mRGC death in comparison with the lower dose. Therefore, the optimal inhibitory effect on the alleviation of H_2O_2-induced cell death is pretreatment with HF at an approximate dose of 50 μg/ml. Taken together our results demonstrated that HF possesses a substantial protective ability against H_2O_2-induced mRGC cell death in the progression of DR.

3.6. HF suppressed H_2O_2-induced mRGC cell apoptosis

To further confirm the protective action of HF against H_2O_2-triggered mRGC cell apoptosis, flow cytometric analysis of mRGC cell double-stained with Annexin V/7-AAD was performed to unveil whether any early or late apoptotic mRGC cell with different interventions (Fig. 5E). The exposure to 0.236 mM H_2O_2 alone elicited an significant increasing apoptotic rate (average early and late apoptotic rate: 2.9% and 18.4%), compared with untreated (1.9% and 1.2%) or pretreated cells at low (3.1% and 1.9%) or high dose (2.4% and 1.6%) of HF (Fig. 5F–I). HF pretreatment with either low or high dose for 24 h could promote the quantity of viable mRGC cells, as well as reduce necrotic cells in comparison with the H_2O_2 alone treatment. Therefore, we postulate that HF acts as a pivotal role in repressing the mRGC cell apoptosis, especially presenting a considerable inhibitory effect on the increase of late-apoptotic mRGC.

3.7. HF inhibited Caspase-3 activity and ROS production in H_2O_2-stressed mRGC cell

The caspase-dependent cascade activation is identified as one of the most characteristic events in the mitochondria-related apoptosis pathway (Kumar et al., 2017). Caspase-3, a member of cysteine protease family, is fully activated in the execution of programmed cell apoptosis (Ghavami et al., 2009). The colorimetric assay of caspase-3 was utilized to determine whether caspase-3 cleavage was in the involvement of H_2O_2-induced mRGC cell apoptosis. As shown in Fig. 4J,

pretreatment with low (OD: 0.074 ± 0.007) or high dose (OD: 0.068 ± 0.003) of HF for 24 h was confirmed to significantly attenuate the activation of cleaved caspase-3, compared with untreated (OD: 0.066 ± 0.003) or H_2O_2-treated mRGC cell (OD: 0.107 ± 0.005) for 48 h. These outcomes further elucidated that HF had an inhibitory effect on mRGC cell apoptosis via repressing caspase-3 activity.

An excessive amount of ROS generation is recognized as a convinced hallmark of oxidative stress in the pathogenesis of DR, which can be initiated by overproduction of H_2O_2 (Newsholme et al., 2016). It revealed that H_2O_2 remarkably enhanced ROS production in mRGCs compared with untreated cells, whereas significant repression of ROS is elicited under HF pretreatment for 24 h (Fig. 5K). This indicates that HF could efficiently prevent H_2O_2-induced mRGC apoptosis at least partly due to its anti-oxidant effect via decrease of ROS production.

3.8. HF alleviated H_2O_2-triggered endoplasmic reticulum- or mitochondria-dependent stress in mRGC cell

Accumulating evidence elucidated that chronic exposure of H_2O_2 could contribute to cell apoptosis in response to endoplasmic reticulum- or mitochondria-dependent stress (Liu et al., 2017a; Ye et al., 2014). It is a noticeable strategy to unveil the assumed pro-survival role of HF against H_2O_2-induced mRGC apoptosis in DR. We further investigated the expressions of endogenous endoplasmic reticulum- or mitochondria-dependent protein, such as phospho-p38 MAPK, ATF4 and CHOP proteins. As shown in Fig. 6A, by comparison to the H_2O_2-treated cells for 48 h, phosphor-p38 MAPK, ATF4 and CHOP proteins (Fig. 6B–D) were significantly down-regulated by either low or high dose of HF pretreatment for 24 h. Concomitantly, high-dose HF administration remarkably improved the expressions of Bcl-XL and Bcl-2 (Fig. 6E–F) proteins. These aforementioned findings suggested that a potential participation of both endoplasmic reticulum- and mitochondria-dysfunction activated proteins in the reversible progression of H_2O_2-induced mRGC cell apoptosis by HF in DR.

3.9. HF restored H_2O_2-induced loss of postsynaptic protein PSD-95 in mRGCs

PSD-95, a membrane-associated guanylate kinase, is a critical postsynaptic scaffolding protein that promotes the stabilization of synaptic contacts as well as neural plasticity in RGC cells (Lam et al., 2016). As compared to untreated or H_2O_2 alone treated cells. HF pretreatment for 24 h could extensively restore the loss of PSD-95 in H_2O_2-stressed cells (Fig. 6G), showing a protective function of HF in inhibiting the decrease of postsynaptic proteins in response to prolonged H_2O_2 exposure to mRGCs.

4. Discussion

Therapeutic strategy designed by searching for safer alternative medicines equipped with multi-target therapy and minimal side effects accelerates the development of novel treatments for DR. Besides exploiting conventional western medicine, herbal formulae taken for diversified medicinal reasons on the basis of clinical efficiency are increasingly popular and deemed to encompass advantage of innately safe to a certain extent (More et al., 2017). Although the neuroprotective mechanisms of HF on oxidative stress and endoplasmic reticulum- induced retinal degeneration have not been thoroughly elaborated, several findings in which we have addressed are demonstrated in the present study. Intensive exposure of H_2O_2 considerably reduced the survival number of mRGCs, while such pathological change could be reversed via HF treatment, indicating the neuroprotective property of HF on DR treatment. Moreover, redundant ROS generation is characterized by the substantial impact on the progression of DR and subsequently caused microvascular disease due to the imbalanced correlation between pro- and anti-oxidants (Fan et al., 2016; Lam et al.,

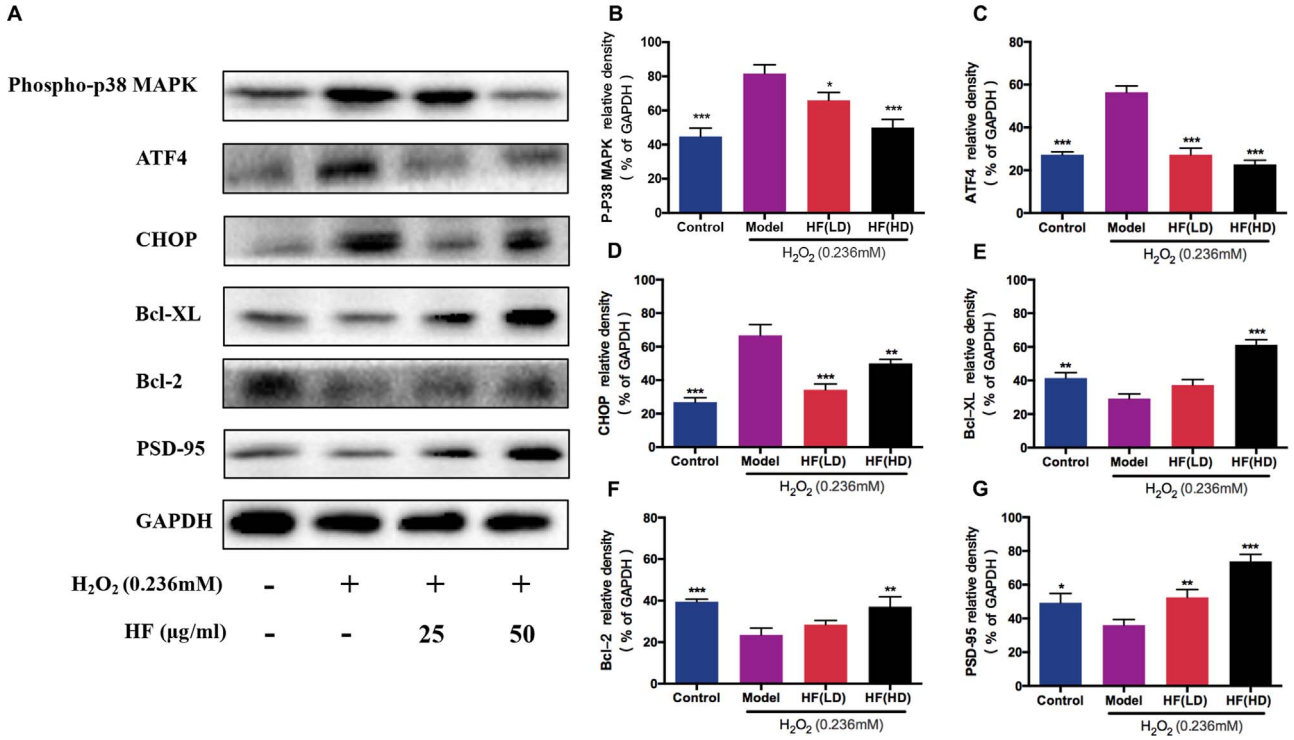

Fig. 6. HF suppressed H2O2-triggered mRGC cell apoptosis via mediating endoplasmic reticulum- or mitochondria-dependent protein expressions. (A) Expression of phospho-p38 MAPK, ATF4, Bcl-XL, Bcl-2, CHOP, PSD-95, GAPDH at protein levels in mRGC cells. Cells were treated in the presence of 0.236 mM H_2O_2 (model) or not (Control) for 48 h. Otherwise, cells were either pretreated with low (LD) or high dose (HD) of HF for 24 h followed by 0.236 mM H_2O_2 exposure for another 24 h. (B, C, D, E, F, G) Bar charts show the mean intensity of each protein quantified and normalized relative to GAPDH expression. Values are presented as mean ± S.D. based on independent experiments in triplicate. HF (LD): HF 25 μg/ml; HF (HD): HF 50 μg/ml. (*) $P < 0.05$, (**) $P < 0.01$ and (***) $P < 0.001$ versus model.

2016; Li et al., 2015). It is particularly worth mentioning that the H_2O_2-induced ROS production is greatly attenuated in HF-treated mRGCs, as illustrated by the declined intensity of DCFDA fluorescence. Thus, our data indicated that HF was observed as an neuroprotectant coupled with the promotion of anti-oxidative activity in the intracellular compartment.

Another noteworthy factor is that mitochondrial dysfunction may account for the main source of ROS production and contribute to DR progression, but it is no longer considered as a sole etiology. Accumulated ROS could lead to the activation of endoplasmic reticulum stress, whereas long-term endoplasmic reticulum stress, containing the presence of excessive H_2O_2, could further generate ROS owing to the stimulation of CHOP-mediated apoptosis accompanied with mitochondria-dependent cell death stimuli (Wang et al., 2016). As shown in the previous report, CHOP, a pro-apoptotic transcriptional effector of endoplasmic reticulum stress-induced apoptosis, is responsible for elevated ROS production and strengthen the feedback of apoptosis response due to the up-regulation of Ero-1α expression, regarding as a thiol oxidase for the inducement of ROS generation (Namba et al., 2009). Our in vitro results are in agreement with previous reports illustrating that an inverse correlation between the survival mRGCs and CHOP-associated expressions is unveiled in the induction of overexpression of ROS. More specifically, besides the highly expressed CHOP via H_2O_2 intervention in mRGCs, the expressions of ATF4, phosphorylated p38 MAPK and cleaved caspase-3 were simultaneously enhanced in mRGCs, which were attenuated by HF. ATF4 was regarded as a critical upstream transcription factor of CHOP. Furthermore, ATF4-CHOP-mediated induction of unfolded protein response and genes encoding protein synthesis was confirmed to promote the RGC death (Han et al., 2013). Activation of p38 MAPK has generally been detected not only in the involvement of overloaded intracellular ROS but also spontaneous caspase-3-mediated cell apoptosis (Jameel et al., 2009). Caspase-3, an intracellular cysteine protease, performed as a terminal effector of the mitochondria-dependent apoptotic pathway. As reported, mitochondrial ROS content was elevated in rats exposed to STZ and caspase-3 was concomitantly increased in RGCs (Yang et al., 2013b), which results are consistent with our results determined by caspase-3 colorimetric assay kit. Furthermore, in our present study, pretreatment of mRGCs with HF has confirmed to concomitantly restore the expression of Bcl-2 and Bcl-xL, after undergoing H_2O_2 treatment which might be potentially contributed to the inhibition of cascaded pathological mechanisms in DR mice. On account of the amelioration of apoptosome-mediated caspases-3 cleavage via HF treatment, we might further speculate that HF could prevent the formation of apoptosome, constituted with three major components: mitochondria-derived cytochrome C (Cyt-C), Apaf-1 and protease caspase-9.

RGCs, located in the ganglion cell layer of the retinae, are the output neurons transmitting information on light to image-forming regions in the brain through the integration between the dendrite and synaptic connections. PSD 95, a major postsynaptic scaffolding protein, participated in the synaptic plasticity and protein assembly. According to literatures, the expression of PSD 95 is declined in the disease of neurodegeneration that is in agreement with our present outcomes both in vitro and in vivo (Gylys et al., 2004), indicating that pretreatment with HF results in positive effects on maintaining the level of PSD 95 in H_2O_2-induced cell apoptosis as well as the neuroprotection of surviving population of RGCs with the counter immunostaining of Brn3a and PSD 95 in STZ-treated diabetic mice. Moreover, activation of ATF4, negatively regulates synaptic plastic leading to the repression of synapse genes and cleaved-caspase-3 has been reported to the contribution of the early postsynaptic dendrites dysfunction (D'Amelio et al., 2011; Pasini et al., 2015). Thus, gradual loss of PSD-95 resulted from the H_2O_2 overexpression in mRGCs or STZ-induced pathological stresses in diabetic mice may be ameliorated via HF treatment through inhibiting the activation of endoplasmic reticulum stress or oxidative stress associated pathological components involving cleaved-caspase-3, ATF4 and its downstream substrate CHOP.

Interestingly, in our study, HF elicited fluctuating hypoglycemic action and not as potent as insulin done in diabetic mice. While insulin-treated diabetic mice undergone progressive vascular degeneration, as similar to the untreated DR mice, which is in agreement with previous reports that intensive insulin therapy contributed to the aggravation of retinal neovascularization in DR, possibly via up-regulating the expression of insulin-like growth factor-1 (IGF-1), hypoxia-inducible factor 1a (HIF-1α) and VEGF (Kaya et al., 2013; Mao et al., 2017). Genetic suppression of ATF4 activity attenuated diabetic-caused retinal vascular leakage and neovascularization associated with enriched avascular fields (Chen et al., 2012; Zeng et al., 2013). Overexpression of oxidized and glycated low-density lipoprotein (HOG-LDL) is implicated in apoptotic pericytes loss by the activation of CHOP-mediated endoplasmic reticulum- or oxidative-stress (Fu et al., 2012). Herein, induction of ATF4 and CHOP pathway might promote the increased E/P ratio in combination with neurovasculopathy in DR mice, which, however, could be alleviated via HF treatment.

Increasing circumstantial evidence of histological material has revealed that RGCs deemed to be lost in patients and mice with DR (Kern and Barber, 2008; Yang et al., 2012). Moreover, the massive absence of RGCs might further correlate with reduction of inner retinal layers in DR and contribute to vision loss (Shimazawa et al., 2012). Our findings were inconsistent with previous reports showing that a cumulative decrease in the quantity of RGCs combined with elevated expression of CHOP immunostaining was demonstrated in DR mice, and associated with the reduction of H&E stained GCL, INL, and IPL, which, however, was alleviated via HF treatment. Activation of ER stress in the early stage of DR resulted in adverse effect on RGC population, contributing to the onset of RGC apoptosis, and was subsequently responsible for RGC loss in DR mice (van Dijk et al., 2009). In addition, increasing in C/ERB homologous- or caspase-dependent protein, involving ATF4, CHOP and caspase-3, were reported to act as a positive role in the neuronal loss as well as retinal microvascular abnormalities in DR (Kowluru and Koppolu, 2002; Yang et al., 2013c), which might further give rise to the changes of pathomorphology and functional disorders in the retinae. Remarkably, thinning of inner retina, especially in IPL, is specifically correlated with gradual loss of neural dendrites and synapses (Barber et al., 1998), probably concomitant with the decrease of PSD 95 as illustrated in the present study.

5. Conclusion

Taken aforementioned findings in the study, originating from both in vitro and in vivo experiments, schematic with hypothetical mechanisms of pharmacological actions of HF against DR were outlined in Fig. 7. It is tempting to ascertain that HF is endowed with multiple protective functions against diabetes-induced RGC apoptosis coupled with retinal microvascular and structural degeneration, such as the destruction of vascular permeability, RGC loss and thinning of inner retinal layer, by scavenging ROS and simultaneously strengthening the attenuation of the activation of ATF4/CHOP-mediated endoplasmic reticulum stress or mitochondria-dependent pro-apoptotic factors, including cleaved-caspase-3, and phosphor-p38 MARK, and subsequently lead to restoration of postsynaptic PSD 95 protein. Meanwhile, the expressions of anti-apoptotic factors like Bcl-2 and Bcl-xL, involved in the prevention of DR, were concomitantly enhanced with the purpose of reinforcing the endogenous defense system. Hereby, HF treatment was convinced to be a novel therapeutic approach not only of alleviating RGC apoptosis but of postponing the onset and progression of DR.

Acknowledgments

The study was partially financial supported by “Fan Ophthalmology of Traditional Chinese Medicine” (Project code: ZY3-CCCX-1-2004),

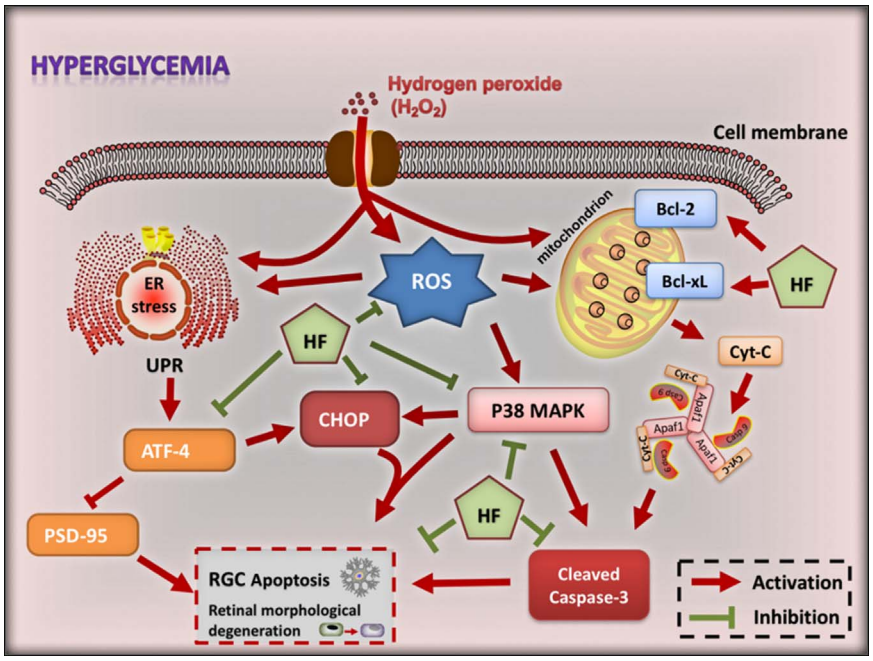

Fig. 7. Proposed schematic of a diabetes-induced model for the pathophysiologic alterations and neuroprotective mechanisms of HF on DR, illustrating respective underlying pathways in relation to alleviate DR progression.

scientific and technological research project of Shanghai Municipal Science and Technology Commission (Project code: 17401970700), grants from the research council of the University of Hong Kong (Project codes: 104003422, 104004092, 104004460), the Research Grants Committee (RGC) of Hong Kong, HKSAR (Project codes: 766211, 17152116), Gala Family Trust (Project code: 200007008), and Government-Matching Grant Scheme (Project code: 207060411).

Author contributions

Yibin Feng and Yinjian Zhang conceived and designed the experiments. Cheng Zhang conducted the experiments and draft the paper. Yu Xu, Sha Li, Hor-Yue Tan, Ning Wang conducted part experiments and analyzed the data. All authors revised the paper and approved the final manuscript.

Conflicts of interest

The authors declare no conflict of interests.

Appendix A. Supporting information

Supplementary data associated with this article can be found in the online version at http://dx.doi.org/10.1016/j.jep.2017.12.018

References

Adamiec-Mroczek, J., Zajac-Pytrus, H., Misiuk-Hojlo, M., 2015. Caspase-dependent apoptosis of retinal ganglion cells during the development of diabetic retinopathy. Adv. Clin. Exp. Med. 24, 531–535.
Barber, A.J., Lieth, E., Khin, S.A., Antonetti, D.A., Buchanan, A.G., Gardner, T.W., 1998. Neural apoptosis in the retina during experimental and human diabetes. Early onset and effect of insulin. J. Clin. Investig. 102, 783–791.
Chen, Y., Wang, J.J., Li, J., Hosoya, K.I., Ratan, R., Townes, T., Zhang, S.X., 2012. Activating transcription factor 4 mediates hyperglycaemia-induced endothelial inflammation and retinal vascular leakage through activation of STAT3 in a mouse model of type 1 diabetes. Diabetologia 55, 2533–2545.
Choi, J.A., Kim, H.W., Kwon, J.W., Shim, Y.S., Jee, D.H., Yun, J.S., Ahn, Y.B., Park, C.K., Ko, S.H., 2017. Early inner retinal thinning and cardiovascular autonomic dysfunction in type 2 diabetes. PLoS One 12, e0174377.
Cui, Y., Wu, J., LI, Y., 2009. Influence of Si MiaoYong An decoction on VEC, ET and inflammatoryfactors of diabetic foot syndrome. Henan J. Tradit. Chin. Med. 29, 151–152.
D'Amelio, M., Cavallucci, V., Middei, S., Marchetti, C., Pacioni, S., Ferri, A., Diamantini, A., De Zio, D., Carrara, P., Battistini, L., Moreno, S., Bacci, A., Ammassari-Teule, M., Marie, H., Cecconi, F., 2011. Caspase-3 triggers early synaptic dysfunction in a mouse model of Alzheimer's disease. Nat. Neurosci. 14, 69–76.
Fan, Y., Qiao, Y., Huang, J., Tang, M., 2016. Protective effects of panax notoginseng saponins against high glucose-induced oxidative injury in rat retinal capillary endothelial cells. Evid.-Based Complement. Altern. Med.: eCAM 2016, 5326382.
Fu, D., Wu, M., Zhang, J., Du, M., Yang, S., Hammad, S.M., Wilson, K., Chen, J., Lyons, T.J., 2012. Mechanisms of modified LDL-induced pericyte loss and retinal injury in diabetic retinopathy. Diabetologia 55, 3128–3140.
Ghavami, S., Hashemi, M., Ande, S.R., Yeganeh, B., Xiao, W., Eshraghi, M., Bus, C.J., Kadkhoda, K., Wiechec, E., Halayko, A.J., Los, M., 2009. Apoptosis and cancer: mutations within caspase genes. J. Med. Genet. 46, 497–510.
Gylys, K.H., Fein, J.A., Yang, F.S., Wiley, D.J., Miller, C.A., Cole, G.M., 2004. Synaptic changes in Alzheimer's disease-Increased amyloid-beta and gliosis in surviving terminals is accompanied by decreased PSD-95 fluorescence. Am. J. Pathol. 165, 1809–1817.
Han, J., Backa, S.H., Hur, J., Lin, Y.H., Gildersleeve, R., Shan, J.X., Yuan, C.L., Krokowski, D., Wang, S.Y., Hatzoglou, M., Kilberg, M.S., Sartor, M.A., Kaufman, R.J., 2013. ER-stress-induced transcriptional regulation increases protein synthesis leading to cell death. Nat. Cell Biol. 15, 481–490.
Hetz, C., 2012. The unfolded protein response: controlling cell fate decisions under ER stress and beyond. Nat. Rev. Mol. Cell Biol. 13, 89–102.
Jameel, N.M., Thirunavukkarasu, C., Wu, T., Watkins, S.C., Friedman, S.L., Gandhi, C.R., 2009. p38-MAPK- and Caspase-3-mediated superoxide-induced apoptosis of rat hepatic stellate cells: reversal by retinoic acid. J. Cell Physiol. 218, 157–166.
Jia, W.C., Liu, G., Zhang, C.D., Zhang, S.P., 2014. Formononetin attenuates hydrogen peroxide (H2O2)-induced apoptosis and NF-kappa B activation in RGC-5 cells. Eur. Rev. Med. Pharmacol. Sci. 18, 2191–2197.
Kaya, A., Kar, T., Aksoy, Y., Ozalper, V., Basbug, B., 2013. Insulin analogues may accelerate progression of diabetic retinopathy after impairment of inner blood-retinal barrier. Med. Hypotheses 81, 1012–1014.
Kern, T.S., Barber, A.J., 2008. Retinal ganglion cells in diabetes. J. Physiol.-Lond. 586, 4401–4408.
Kim, J.M., Hong, K.S., Song, W.K., Bae, D., Hwang, I.K., Kim, J.S., Chung, H.M., 2016. Perivascular progenitor cells derived from human embryonic stem cells exhibit functional characteristics of pericytes and improve the retinal vasculature in a rodent model of diabetic retinopathy. Stem Cell Transl. Med. 5, 1268–1276.
Kowluru, R.A., Koppolu, P., 2002. Diabetes-induced activation of caspase-3 in retina: effect of antioxidant therapy. Free Radic. Res. 36, 993–999.
Kumar, S., Eroglu, E., Stokes, J.A., Scissum-Gunn, K., Saldanha, S.N., Singh, U.P., Manne, U., Ponnazhagan, S., Mishra, M.K., 2017. Resveratrol induces mitochondria-mediated, caspase-independent apoptosis in murine prostate cancer cells. Oncotarget 8, 20895–20908.
Lam, P., Cheung, F., Tan, H.Y., Wang, N., Yuen, M.F., Feng, Y.B., 2016. Hepatoprotective effects of Chinese medicinal herbs: a focus on anti-inflammatory and anti-oxidative activities. Int. J. Mol. Sci. 17, 465.
Lee, R., Wong, T.Y., Sabanayagam, C., 2015. Epidemiology of diabetic retinopathy, diabetic macular edema and related vision loss. Eye Vis 2, 17.
Li, S., Tan, H.Y., Wang, N., Zhang, Z.J., Lao, L., Wong, C.W., Feng, Y., 2015. The role of oxidative stress and antioxidants in liver diseases. Int. J. Mol. Sci. 16, 26087–26124.
Liu, X.R., Cao, L., Li, T., Chen, L.L., Yu, Y.Y., Huang, W.J., Liu, L., Tan, X.Q., 2017a. Propofol attenuates H2O2-induced oxidative stress and apoptosis via the mitochondria- and ER-medicated pathways in neonatal rat cardiomyocytes. Apoptosis 22,

639–646.
Liu, Z., Zhang, Y., Zhang, R., Gu, L., Chen, X., 2017b. Promotion of classic neutral bile acids synthesis pathway is responsible for cholesterol-lowing effect of Si-miao-yong-an decoction: application of LC-MS/MS method to determine 6 major bile acids in rat liver and plasma. J. Pharm. Biomed. Anal. 135, 167–175.
Mao, X.B., You, Z.P., Wu, C., Huang, J., 2017. Potential suppression of the high glucose and insulin-induced retinal neovascularization by Sirtuin 3 in the human retinal endothelial cells. Biochem. Biophys. Res. Commun. 482, 341–345.
More, S.V., Kim, I.S., Choi, D.K., 2017. Recent update on the role of Chinese material Medica and formulations in diabetic retinopathy. Molecules 22.
Nadal-Nicolas, F.M., Jimenez-Lopez, M., Sobrado-Calvo, P., Nieto-Lopez, L., Canovas-Martinez, I., Salinas-Navarro, M., Vidal-Sanz, M., Agudo, M., 2009. Brn3a as a marker of retinal ganglion cells: qualitative and quantitative time course studies in naive and optic nerve-injured retinas. Investig. Ophthalmol. Vis. Sci. 50, 3860–3868.
Namba, T., Tanaka, K., Ito, Y., Ishihara, T., Hoshino, T., Gotoh, T., Endo, M., Sato, K., Mizushima, T., 2009. Positive role of CCAAT/Enhancer-binding protein homologous protein, a transcription factor involved in the endoplasmic reticulum stress response in the development of colitis. Am. J. Pathol. 174, 1786–1798.
Newsholme, P., Cruzat, V.F., Keane, K.N., Carlessi, R., de Bittencourt, P.I.H., 2016. Molecular mechanisms of ROS production and oxidative stress in diabetes. Biochem. J. 473, 4527–4550.
Ng, D.S.K., Chiang, P.P.C., Tan, G., Cheung, C.M.G., Cheng, C.Y., Cheung, C.Y., Wong, T.Y., Lamoureux, E.L., Ikram, M.K., 2016. Retinal ganglion cell neuronal damage in diabetes and diabetic retinopathy. Clin. Exp. Ophthalmol. 44, 243–250.
Pasini, S., Corona, C., Liu, J., Greene, L.A., Shelanski, M.L., 2015. Specific downregulation of hippocampal ATF4 reveals a necessary role in synaptic plasticity and memory. Cell Rep. 11, 183–191.
Sano, R., Reed, J.C., 2013. ER stress-induced cell death mechanisms. Bba-Mol. Cell Res. 1833, 3460–3470.
Shimazawa, M., Miwa, A., Ito, Y., Tsuruma, K., Aihara, M., Hara, H., 2012. Involvement of endoplasmic reticulum stress in optic nerve degeneration following N-methyl-D-aspartate-induced retinal damage in mice. J. Neurosci. Res. 90, 1960–1969.
Singh, R.S.J., Covert, D.J., Henry, C.R., Bhatia, S.K., Croskrey, J., Sanchez, C.R., Han, D.P., 2014. Retinal complications associated with pars plana vitrectomy for macular holes or epiretinal membranes in eyes with previous retinal detachment repair. JAMA Ophthalmol. 132, 118–119.
Tremolada, G., Del Turco, C., Lattanzio, R., Maestroni, S., Maestroni, A., Bandello, F., Zerbini, G., 2012. The role of angiogenesis in the development of proliferative diabetic retinopathy: impact of intravitreal anti-VEGF treatment. Exp. Diabetes Res. 728325.
van Dijk, H.W., Kok, P.H.B., Garvin, M., Sonka, M., DeVries, J.H., Michels, R.P.J., van Velthoven, M.E.J., Schlingemann, R.O., Verbraak, F.D., Abramoff, M.D., 2009. Selective loss of inner retinal layer thickness in type 1 Diabetic patients with minimal diabetic retinopathy. Investig. Ophthalmol. Vis. Sci. 50, 3404–3409.
van Dijk, H.W., Verbraak, F.D., Kok, P.H.B., Garvin, M.K., Sonka, M., Lee, K., DeVries, J.H., Michels, R.P.J., van Velthoven, M.E.J., Schlingemann, R.O., Abramoff, M.D., 2010. Decreased retinal ganglion cell layer thickness in patients with type 1 diabetes. Investig. Ophthalmol. Vis. Sci. 51, 3660–3665.
Wang, D.D., Zhu, H.Z., Li, S.W., Yang, J.M., Xiao, Y., Kang, Q.R., Li, C.Y., Zhao, Y.S., Zeng, Y., Li, Y., Zhang, J., He, Z.D., Ying, Y., 2016. Crude saponins of panax notoginseng have neuroprotective effects to inhibit palmitate-triggered endoplasmic reticulum stress-associated apoptosis and loss of postsynaptic proteins in staurosporine differentiated RGC-5 retinal ganglion cells. J. Agric. Food Chem. 64, 1528–1539.
Wang, L.L., Wang, N., Tan, H.Y., Zhang, Y.J., Feng, Y.B., 2015. Protective effect of a Chinese Medicine formula He-Ying-Qing-Re Formula on diabetic retinopathy. J. Ethnopharmacol. 169, 295–304.
Watal, G., Dhar, P., Srivastava, S.K., Sharma, B., 2014. Herbal medicine as an alternative medicine for treating diabetes: the global burden. Evid.-Based Complement. Alt.
Whiting, D.R., Guariguata, L., Weil, C., Shaw, J., 2011. IDF Diabetes Atlas: global estimates of the prevalence of diabetes for 2011 and 2030. Diabetes Res. Clin. Pract. 94, 311–321.
Xu, C.Y., Bailly-Maitre, B., Reed, J.C., 2005. Endoplasmic reticulum stress: cell life and death decisions. J. Clin. Investig. 115, 2656–2664.
Yang, C., Yuan, Z., Zhang, J., 2013a. Study on the effects of Simiao yong an decoction on the vascular smooth muscle cell migration. Chin. J. Tradit. Chin. Med. Pharm. 28, 1480–1483.
Yang, J.H., Kwak, H.W., Kim, T.G., Han, J., Moon, S.W., Yu, S.Y., 2013b. Retinal neurodegeneration in type II diabetic Otsuka long-evans Tokushima fatty rats. Investig. Ophthalmol. Vis. Sci. 54, 3844–3851.
Yang, L., Wu, L., Wang, D., Li, Y., Dou, H., Tso, M.O., Ma, Z., 2013c. Role of endoplasmic reticulum stress in the loss of retinal ganglion cells in diabetic retinopathy. Neural Regen. Res. 8, 3148–3158.
Yang, Y., Liu, Q., 2008. Clinical trial of combination of six ingredient Rehmannia pill and Si-miao-yong-An Decoction on diabetic retinopathy. ShenZhen J. Inter. Tradit. Chin. West Med. 18, 300–301.
Yang, Y., Mao, D., Chen, X., Zhao, L., Tian, Q., Liu, C., Zhou, B.L., 2012. Decrease in retinal neuronal cells in streptozotocin-induced diabetic mice. Mol. Vision. 18, 1411–1420.
Ye, C., Zhang, Y., 2012. Clinical observation of harmonizing ying and clearing heat therapy on diabetic retinopathy in non proliferative stage. Hebei J. Tradit. Chin. Med. 34, 1204–1205.
Ye, J.L., Han, Y.T., Chen, X.H., Xie, J., Liu, X.J., Qiao, S.H., Wang, C.B., 2014. L-carnitine attenuates H2O2-induced neuron apoptosis via inhibition of endoplasmic reticulum stress. Neurochem. Int. 78, 86–95.
Zeng, L., Tallaksen-Greene, S.J., Wang, B., Albin, R.L., Paulson, H.L., 2013. The de-ubiquitinating enzyme ataxin-3 does not modulate disease progression in a knock-in mouse model of Huntington disease. J. Huntingt. Dis. 2, 201–215.
Zhang, J., XU, Y., LI, M., LI, L., Pang, L., Zhang, G., Yang, C., Zhou, Y., 2010. Effect of Simiao yong an decoction on oxidative stress and inflammation on atherosclerosis model rabbits. J. Tradit. Chin. Med. 51, 72–74.
Zhang, K.Z., Kaufman, R.J., 2004. Signaling the unfolded protein response from the endoplasmic reticulum. J. Biol. Chem. 279, 25935–25938.
Zhang, Y., Su, J., LI, H., Ruan, W., Liu, X., Ye, C., Zou, J., 2012. Combination of “Heying prescription” and laser therapy for diabetic retinopathy. Shanghai J. Tradit. Chin. Med. 46, 50–52.